Check for updates

Acrylate–methacrylate radical copolymerization kinetics of sparingly water-soluble monomers in polar and nonpolar solvents†

Noushin Rajabalinia, [ID] Fatemeh Salarhosseini and Robin A. Hutchinson [ID] *

The properties of waterborne polymer dispersions synthesized by emulsion radical polymerization are influenced by reactions in both the aqueous medium and the growing particles. Mathematical models representing the process often do not consider the difference in the propagation rate coefficient (k_p) of monomers in the two phases, despite the body of evidence demonstrating that solvent polarity influences monomer–monomer and monomer-solvent hydrogen-bonding that affects both k_p homopropagation values and copolymerization reactivity ratios. Therefore, it is vital to develop experimental approaches to systematically measure the influence of solvent on the copolymerization kinetics of hydrophobic monomers under conditions that are similar to emulsion systems. In this work, we study the copolymerization of methyl acrylate (MA) with di(ethylene glycol) methyl ether methacrylate (DEGMEMA) as models for the common emulsion monomers butyl acrylate and methyl methacrylate. As well as varying solvent choice and monomer concentration, MA/DEGMEMA copolymerization kinetics are compared to those of MA with methacrylic acid (MAA) to determine the influence of monomer functionality on its relative reactivity. The findings suggest that the copolymer composition of all methacrylate–acrylate systems – whether involving functional or non-functional monomers – converge to a single curve in protic polar aqueous solution.

Introduction

Waterborne polymer dispersions, used in a broad range of industries[1] including (meth)acrylate dispersions for coatings and adhesives,[2] are mostly synthesized by emulsion radical polymerization *via* a complex polymerization mechanism. Although most polymer formation occurs within the dispersed particles, reactions in the aqueous medium play an important role in controlling particle nucleation and radical entry into the particles.[3] Despite the commercial importance of producing dispersions with desired performance characteristics, unsolved issues remain that prevent detailed kinetic models from capturing all of the important features of the process.[4] In particular, the current understanding and mathematical models fail to accurately represent particle nucleation and the resulting particle size distribution of the synthesized polymer dispersions.[5] Some of these difficulties arise from an inadequate treatment of the kinetics of chain growth in the aqueous phase.

Using a water-soluble initiator, the initial chain growth of newly formed radicals occurs in the aqueous medium[6] under conditions for which the propagation coefficient rate (k_p) describing the addition of the sparingly-soluble monomer to the growing oligomers is chain-length dependent (CLD).[7] Oligomer growth in the water continues until the growing chain either enters a micelle or polymer particle,[6,8] or reaches a critical chain length and becomes insoluble in water by the process known as homogeneous nucleation.[9] Despite significant efforts to develop first-principle representations of radical entry[10,11] to and radical exit[5] from the particles, their reliability is still debatable[12] because of the lack of accounting for the CLD and/or solvent dependency of k_p in water compared to in the particles.

A significant body of work has emerged using specialized pulsed-laser polymerization techniques to demonstrate that solvent polarity can significantly affect chain growth,[13,14] with the k_p of water-soluble monomers more than a magnitude higher in water compared to in organic media;[15] *i.e.*, within the growing polymer particles. However, less is known about the influence of water on the propagation kinetics of monomers with limited solubility in aqueous solution, such as those typically used in emulsion polymerization. Agboluaje *et al.* compared the relative influence of polar solvents – both alcohols and water – on k_p values of sparingly soluble non-

Department of Chemical Engineering, Queen's University, 19 Division St., Kingston, ON K7L 3N6, Canada. E-mail: robin.hutchinson@queensu.ca

†Electronic supplementary information (ESI) available. See DOI: https://doi.org/10.1039/d4py01015a

functional 2-methoxyethyl acrylate (MEA) and methyl acrylate (MA) to that of fully water-soluble acrylic acid (AA).[16] While transitioning from bulk to solution polymerization with 5–10 wt% of monomer in alcohol resulted in a 2-fold k_p increase for MA and MEA, the value for AA decreased by a factor of 2. The difference in behavior was explained by competitive hydrogen bonding effects: alcohol enhances the reactivity of the non-functional acrylates through H-bonding with monomer but reduces the reactivity of AA by disruption of the monomer dimerization that occurs in bulk. On the other hand, it was found that k_p for 5 wt% MA, MEA and AA in water was 16, 8, and 4.6 times higher than bulk, respectively, with the values for the three monomers converging to 160–200 × 10^3 L mol^{-1} s^{-1} at 25 °C.[16] This difference in the relative influence of water on the propagation of non-functional and functional monomers is expected to be important for emulsion systems, which often involves the copolymerization of monomers with limited water solubility (*e.g.*, styrene, butyl acrylate, methyl methacrylate) with water-soluble functional monomers (*e.g.*, 2-hydroxyethyl (meth)acrylate, (meth)acrylic acid).[17]

As homopropagation k_p values of functional and non-functional monomers show different sensitivities towards water, it is not surprising that solvent nature also affects the reactivity ratios of monomers in radical copolymerization and thus copolymer composition, as has been reported for methyl methacrylate (MMA) copolymerized with methacrylic acid (MAA)[18] and AA[19] in a variety of organic solvents. More recently, Agboluaje *et al.* demonstrated that the relative incorporation of 2-hydroxyethyl methacrylate (HEMA) into HEMA/MEA copolymer is reduced in alcohols and methanol–water mixtures compared to the copolymer synthesized in bulk,[20] as also found for HEMA copolymerized with butyl methacrylate (BMA)[21] and 2-hydroxyethyl acrylate (HEA) copolymerized with both butyl acrylate (BA)[22] and BMA.[23] The HEMA/MEA study also demonstrated that solvent polarity had a much stronger influence on the composition-averaged propagation rate coefficient in the system (*i.e.*, polymerization rate) than on the system reactivity ratios (*i.e.*, copolymer composition).[20] Deglmann *et al.* computationally studied the effect of medium on copolymer composition, demonstrating that the experimental variations in reactivity ratios with solvent choice are captured by considering thermodynamic nonidealities, as captured by the activity coefficients of the two monomers and transition states involved.[24]

With regards to emulsion system, the time required for an oligomer to reach a critical chain growth will depend both on chain growth rates and copolymer composition, as the difference in the hydrophobicity of comonomers influences oligomeric solubility and thus radical entry.[25] While the emulsion copolymerization of MMA and BA has been widely studied due to its wide application as coatings and adhesives,[26] to the best of our knowledge their reactivity ratios in aqueous solution have not been measured due to their hydrophobicity. In this work we take the first steps to determining these values under conditions as similar as possible to those in the aqueous phase of emulsion polymerization. Our strategy is to substitute
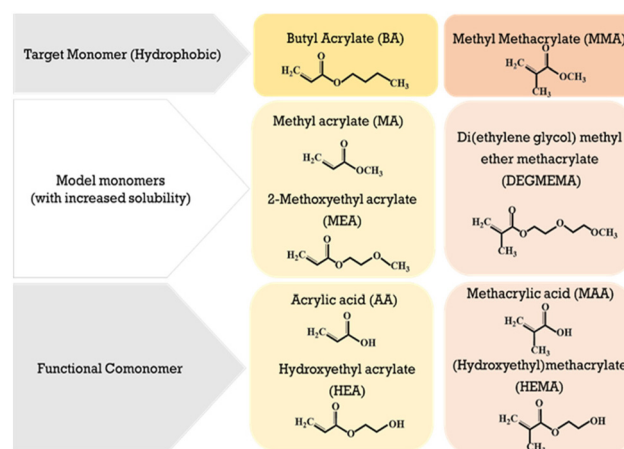
Fig. 1 Acrylate and methacrylate monomers selected to gain insight on aqueous-phase kinetics of commercial BA–MMA emulsion copolymerization as well as the influence of adding functional comonomers to the system.

MMA and BA with non-functional monomers of similar structure but with increased water solubility, as shown in Fig. 1. With a water solubility of ~5 wt%, MA is a natural substitute for BA, and we select di(ethylene glycol) methyl ether methacrylate (DEGMEMA) as a non-functional methacrylate with increased water solubility (~6 wt%) compared to MMA. These selections are based upon our previous findings that the influence of solvent polarity on the reactivity of non-functional monomers is similar (*e.g.*, MEA *vs.* MA[16] and MEA *vs.* BA[22]).

In addition to our interest on the influence of solvent on MA/DEGMEMA copolymerization, we would like to quantify the influence of monomer functionality on relative reactivity during the transition from non-polar to polar solvents. Both hydroxy-functional (HEA and HEMA) and acid functional (AA and MAA) monomers are commonly added to many emulsion systems. Thus, we compare the combined influence of solvent selection and methacrylate functionality on the relative reactivities of MA/MAA and MA/DEGMEMA. *In situ* NMR is used to track individual monomer consumption rates up to high conversion, thus providing a measure of both reaction rate (*i.e.*, overall rate of conversion) and of the system reactivity ratios (estimated from the relative rates of comonomer consumption).

Experimental section

Materials

All chemicals in this study were used as received without further purification. Methyl acrylate [MA] (99%, contains ≤100 ppm monomethyl ether hydroquinone [MEHQ] as inhibitor, Sigma-Aldrich), methacrylic acid [MAA] (99% contains 250 ppm MEHQ, Aldrich), di(ethylene glycol) methyl ether methacrylate [DEGMEMA] (95%, Aldrich), 2,2′-azobis(2-methylpropionitrile) [AIBN] (98%, Aldrich), 2,2′-azobis(2-methylpropionamidine) dihydrochloride [V-50] (97%, Aldrich), 1,3,5-trioxane (99%, Tokyo Chemical Industry Co., Ltd), dimethyl

sulfoxide-d$_6$ [DMSO-d$_6$] (99.5% isotropic, Thermo Scientific), toluene-d$_8$ (99.5% atom D, Cambridge Isotope Laboratories, Inc.), ethanol-d$_1$ [EtOD, C$_2$H$_5$OD] (≥99.5% atom D, Sigma-Aldrich) and deuterium oxide [D$_2$O] (Sigma-Aldrich) were used.

In situ ^{1}H NMR polymerizations

The effect of altering comonomer composition, monomer functionality, solvent type and concentration on compositional drift to high conversion has been studied in the copolymerization of MA with MAA and with DEGMEMA, as summarized in Tables S1 and S2 in ESI.† The initiator was switched from oil-soluble AIBN to water-soluble V-50 when the D$_2$O fraction in D$_2$O/EtOD mixtures was ≥50 wt%.

NMR mixtures were prepared based on the given formulations in Tables S1 and S2† by adding the corresponding amounts of monomers, solvent(s) and initiator to a glass vial at ambient temperature. Each solution was well mixed using a vortex mixer to ensure sample homogeneity. No purging with an inert gas was performed as the presence of small amount of oxygen retards the start of the polymerization, with the inhibition time allowing the tracking of conversion from the start of reaction.[27,28] 0.5–1 ml of each sample was transferred to a Wilmard® 5 mm NMR tube and was stored in the fridge prior to the in situ NMR experiments.

In situ ^{1}H NMR experiments were performed using Bruker 500, 600 and 700 MHz NMR spectrometers equipped with TopSpin 4 NMR processing software. As the focus of the study was the influence of solvent and monomer selection on copolymer composition, and it has been reported that temperature has a negligible effect on acrylate–methacrylate reactivity ratios,[23] all experiments were performed at 60 °C. The NMR sample chamber was equilibrated to the reaction temperature before the samples were inserted. After sample equilibration to the reaction temperature in the chamber, the software was locked to the deuterated defined solvent and the sample was shimmed and tuned within 3 to 5 min of inserting the tube to ensure the quality of the acquired spectra, as sharp peaks and a flat baseline are critical for quantitative analysis of the spectrum. Acquisition parameters were set to a relaxation delay (d1) of 20 s to prevent error arising from peak saturation,[29] with 8 scans per acquisition to provide a spectrum with a good signal to noise ratio every 3–4 min. Each reaction was followed up to the highest attainable monomer conversion (always >65%) without losing spectra quality due to loss of shimming. The reproducibility of the experimental procedure and data analysis was verified by repeating some solvent/comonomer formulations three times. Fig. S1† provides an example set of data collected for MA/MAA (w_{mon} = 0.2) in a mixture containing equal mass fractions of D$_2$O and EtOD (α_{EtOD} = 0.5) for two different initial comonomer compositions ($f_{MA,0}$ = 0.20 and 0.50), plotting both overall monomer conversion (X) vs. time and the evolution of f_{MA} vs. X.

Following the procedures described by Preusser and Hutchinson,[30] the change in comonomer composition with overall monomer conversion as well as the change in overall monomer conversion with time was calculated from the decrease in intensity of distinct peaks corresponding to the two monomers in the system. Details for the specific monomer/solvent systems in the current work are provided in Section S1 to S5 of the ESI.†

Reactivity ratio estimation

The drifts in comonomer composition vs. overall monomer conversions were used to estimate reactivity ratios – i.e., the relative propensy of radical-i to react with monomer-i compared to monomer-j:

$$r_i = \frac{k_{ii}}{k_{ij}}, \, i,j = 1, 2 \tag{1}$$

using the direct numerical integration (DNI) method[31] and the non-linear parameter estimation features in PREDICI by solving the following equation:

$$\frac{df_1}{dX} = \frac{f_1 - F_1^{Inst}}{1 - X}, \, f_1(X = 0) = f_{1,0} \tag{2}$$

where X and f_1 are the paired NMR measurements of overall monomer conversion and mole fraction of monomer 1 (MA) in the comonomer mixture, respectively, and F_1^{Inst} is the instantaneous copolymer composition of MA calculated assuming terminal model kinetics:

$$F_1^{Inst} = \frac{r_1 f_1^2 + f_1 f_2}{r_1 f_1^2 + 2 f_1 f_2 + r_2 f_2^2}, \, f_1 + f_2 = 1 \tag{3}$$

Following the terminology recently introduced by an IUPAC working group on "Experimental Methods and Data Evaluation Procedures for the Determination of Radical Copolymerization Reactivity Ratios",[32] this procedure can be referred to as the f_0–f–X method, as the reactivity ratio estimates determined from the fit of the f vs. X data are also dependent on the values of $f_{1,0}$ specified as the initial condition when solving eqn (2). For all experiments conducted in this study, the $f_{1,0}$ determined in the lab via gravimetry was used in the parameter estimations, with the excellent agreement between the NMR-measured and lab values illustrated by the examples provided in ESI Sections S1–S5.† The r_1 and r_2 values were estimated for each solvent/monomer/comonomer mixture (e.g., MA/MAA with w_{mon} = 0.1 in DMSO-d$_6$) by combining data from three experiments with $f_{1,0}$ set to 0.20, 0.50, and 0.80. We assume that each f_1–X data measurement is independent, as every NMR spectrum is analyzed separately with no dependence on the values determined from the previous spectrum.

The validity of the estimated reactivity ratios using this methodology is checked for some of the data sets by using material balances to estimate cumulative copolymer composition (F_1^{cum}) according to eqn (4):

$$F_1^{cum} = \frac{f_{1,0} - (1 - X) f_1}{X} \tag{4}$$

and then fitting the resulting f_0–F–X data using the Contour software downloaded from the link provided with the IUPAC paper.[32] This methodology accounts for measurement error, with the absolute error in both f_1 and X assumed to be ± 0.01

based on the accuracy of NMR peak integrations and the corresponding error in F_1^{cum} calculated according to standard "propagation of error" methodology.[32] In addition, the same data sets were processed using an Excel macro provided in the same publication that estimates the reactivity ratios by fitting the data to the analytical solution to Skeist's equation (eqn (S8) in ESI†) derived by Meyer and Lowry (ML).[33] The differences in the mean r values and the 95% joint confidence regions (JCR) from the three procedures are minor, as presented for the copolymerization of MA/DEGMEMA in DMSO-d_6 and toluene-d_8 and MA/MAA in DMSO-d_6. These differences, likely arising from the numerical solution algorithms, are small compared to the differences found when changing reaction conditions or monomer systems.

As a further check on both the experimental and estimation procedures, separate JCRs were calculated for the Fig. S1† repeat experiments conducted for MA/MAA in D_2O : EtOD (α_{EtOD} = 0.5) with w_{mon} = 0.2, as shown as Fig. S1(c).† The three JCRs overlap, with the small differences seen related to the range of data covered for the same initial conditions run for varying reaction times: the shorter 40 minute experiments cover a reduced f_1 range compared to those run for longer reaction times to higher conversion. Our approach for subsequent experiments was to follow the reaction to the highest possible overall conversion while still achieving good quality NMR spectra, thus covering a sufficient composition range to ensure the validity of the estimated reactivity ratios.[34]

With these verifications of our methodology, the remaining reactivity ratios reported in this work are determined using the DNI procedure and parameter estimation tools in PREDICI.

Results and discussion

The original plan was to use *in situ* NMR to track MA/DEGMEMA and MA/MAA copolymerization in a series of deuterated solvents progressing from non-polar toluene-d_8 to D_2O, as shown in Fig. 2. However, NMR shimming was not sufficiently stable for some reaction mixtures in toluene-d_8 (*e.g.*, MA/MAA with w_{mon} = 0.1 and 0.5 and MA/DEGMEMA with w_{mon} = 0.5). In addition, it is necessary that the monomer/polymer/solvent system stays homogeneous throughout the complete experiment to have confidence in the data analysis. Thus, some conditions were not fully analyzed due to polymer precipitation that occurred in pure D_2O and D_2O-rich EtOD : D_2O mixtures. Nonetheless, much can be learned by comparing the behavior of the two comonomer systems in non-aqueous and EtOD : D_2O mixtures with increased polarity. Analysis and discussion of the polymerization rates (*i.e.*, monomer conversion profiles) is deferred until

later, as we first focus on comonomer composition drifts and estimation of reactivity ratios.

Copolymerization in non-aqueous solutions

We first compare the MA/MAA and MA/DEGMEMA systems in DMSO-d_6 (w_{mon} = 0.5 and 0.1, C_{AIBN} = 0.2 wt%), also reporting results for MA/DEGMEMA in toluene-d_8 (w_{mon} = 0.1, C_{AIBN} = 2.0 wt%). Fig. 3 compares the evolution of f_{MA} *vs.* X from the copolymerization of MA/DEGMEMA, as measured in toluene-d_8 (w_{mon} = 0.1) and in DMSO-d_6 (w_{mon} = 0.5 and 0.1). In all cases, as expected for a methacrylate–acrylate copolymerization, DEGMEMA is preferentially consumed such that f_{MA} increases with increasing conversion. Moreover, the data sets overlap, following the same trajectories in monomer composition for both solvents and for the two monomer levels in DMSO-d_6. Table 1 summarizes the reactivity ratios estimated from fitting of the three data sets using the three estimation methods. Despite the overlap in the f_{MA} *vs.* X curves, there are minor differences between the best fit mean values of r_{MA} and $r_{DEGMEMA}$ that exceed the reported 95% confidence intervals. The 95% joint confidence region (JCR) ellipsoids calculated by the Excel ML macro and the Contour program are compared in Fig. 4(a) to the 95% confidence intervals (indicated by error
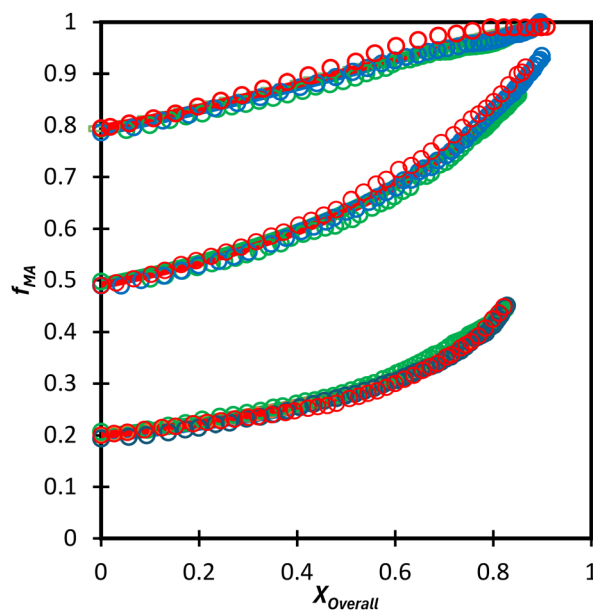

Fig. 3 Drift in MA comonomer composition (f_{MA}) with overall monomer conversion for MA/DEGMEMA in toluene-d_8 with w_{mon} = 0.1 (green) and in DMSO-d_6 with w_{mon} = 0.5 (blue) and 0.1 (red). Symbols are experimental data and lines with same colour are simulated using the overall best-fit reactivity ratios estimated from the combined data set (r_1 = 0.36, r_2 = 2.16).
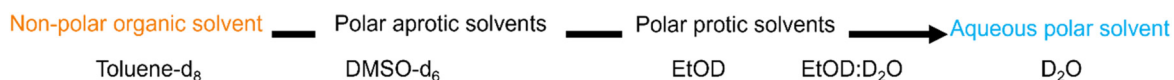
Fig. 2 Target solvents, systematically increasing polarity as solvent is changed from organic to aqueous.

Non-polar organic solvent — Polar aprotic solvents — Polar protic solvents — Aqueous polar solvent

Toluene-d_8 DMSO-d_6 EtOD   EtOD:D_2O D_2O

Table 1 Reactivity ratios (with 95% confidence intervals) for the copolymerization of MA/DEGMEMA in toluene-d_8 and DMSO-d_6 estimated using three different methodologies

Solvent	$w_{mon,0}$	DNI		ML		ML (reduced points)[a]		Contour	
		r_{MA}	$r_{DEGMEMA}$	r_{MA}	$r_{DEGMEMA}$	r_{MA}	$r_{DEGMEMA}$	r_{MA}	$r_{DEGMEMA}$
Toluene-d_8	0.1	0.42 ± 0.01	2.17 ± 0.02	0.43 ± 0.01	2.13 ± 0.02	0.43 ± 0.02	2.08 ± 0.06	0.42 ± 0.01	2.12 ± 0.02
DMSO-d_6	0.5	0.25 ± 0.01	2.03 ± 0.02	0.29 ± 0.01	2.08 ± 0.02	0.29 ± 0.01	2.10 ± 0.05	0.26 ± 0.06	2.02 ± 0.02
DMSO-d_6	0.1	0.36 ± 0.01	2.25 ± 0.02	0.38 ± 0.01	2.22 ± 0.02	0.38 ± 0.01	2.21 ± 0.03	0.37 ± 0.01	2.21 ± 0.01
All three sets	0.36 ± 0.01	2.16 ± 0.02	0.40 ± 0.01	2.18 ± 0.01	0.38 ± 0.01	2.15 ± 0.04	0.38 ± 0.01	2.14 ± 0.02

[a] One data point per 10% overall conversion.

(a)

(b)
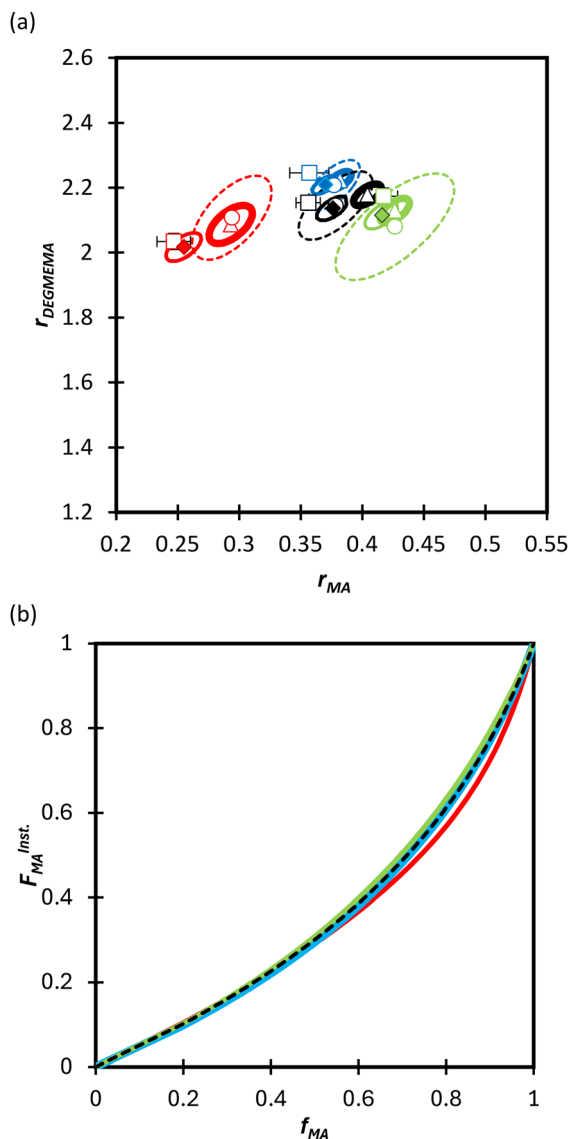
Fig. 4 (a) 95% joint confidence regions from estimation of the reactivity ratios and (b) F_{MA}^{Inst} vs. f_{MA} calculated for the copolymerization of MA/DEGMEMA in toluene-d_8 with w_{mon} = 0.1 (green), in DMSO-d_6 with w_{mon} = 0.5 (red) and 0.1 (blue), and all data combined (black). The JCRs were obtained by different parameter estimation techniques (see Table 1 and text): ML considering all (solid thicker lines with △ indicating best-fit values) and a reduced number of experimental data (dashed lines, ○), Contour (solid thinner lines, ✦), and DNI (□, with error bars). F_{MA}^{Inst} is derived using estimated reactivity ratios from the DNI fit.

bars) for r_{MA} and $r_{DEGMEMA}$ estimated using the DNI method. The plot range in Fig. 4(a) is set to facilitate visual comparison with later results. The size of the uncertainties is similarly very small (*e.g.*, ±0.02) for all three estimation methods, a result related to the large number of experimental points (∼100) in each 3-experiment set collected by the *in situ* NMR method. To explore the sensitivity of the JCR to the size of the data set, the number of points was reduced by a factor of 5 (*i.e.*, from 1 point per every 2% of overall conversion to 1 point per 10% of overall conversion) for the ML fit. While the r_{MA} and $r_{DEGMEMA}$ estimates were unchanged, the JCR increased in area significantly to encompass the reactivity ratio values estimated by both Contour and DNI (Fig. 4a).

Even with the larger JCRs, the r_{MA} estimates from the three DEGMEMA/MA data sets (in DMSO-d_6 with w_{mon} = 0.5 and 0.1 and in toluene-d_8 with w_{mon} = 0.1) do not overlap. Nonetheless, the three data sets are well represented by a single pair of values, r_{MA} = 0.36 ± 0.01 and $r_{DEGMEMA}$ = 2.16 ± 0.02, estimated from a fit of the combined data, as shown by the predicted composition drifts in Fig. 3, with plots of the fit to the individual data sets included as Fig. S7.† In addition, the F_{MA} vs. f_{MA} curve (generated according to eqn (3)) using the best-fit reactivity ratios from the combined data set show very little difference to those generated from the individual fits, as shown in Fig. 4(b). F_{MA} vs. f_{MA} plots comparing each case separately to the overall fit are shown as Fig. S8,† with experimental points added to indicate the range in f_{MA} covered by following the reactions to high conversions. The maximum relative difference in F_{MA} values is 7%, found when comparing the overall fit to the fit for DMSO-d_6 with w_{mon} = 0.5, as might be expected from a visual inspection of the JCRs in Fig. 4(a). Thus, while a variation in the value of r_{MA} with solvent level cannot be ruled out, its influence on comonomer composition drift and corresponding copolymer compositions is small.

Turning our attention to the MA/MAA system, Fig. 5 shows the compositional drift measured in DMSO-d_6 up to high conversion with w_{mon} = 0.5 and 0.1. It is evident that increasing the monomer concentration to w_{mon} = 0.5 increases the relative consumption rate of MAA, as indicated by the sharper increase in f_{MA} with conversion, especially evident for $f_{MA,0}$ = 0.2. The reactivity ratio estimates are summarized in Table 2, with the best-fit curves added to Fig. 5. As found for MA/DEGMEMA and shown in Fig. 6(a), the JCR and mean values from the three parameter estimation methods agree well for each MA/
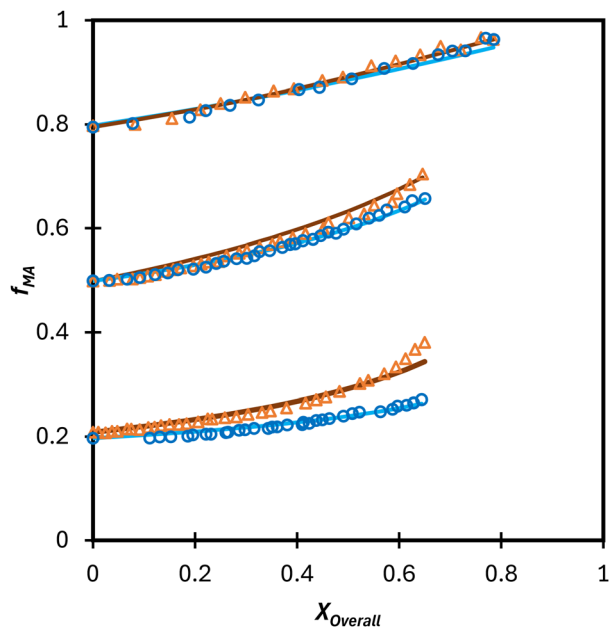
Fig. 5 Drift in MA comonomer composition (f_{MA}) with overall monomer conversion for the copolymerization of MA/MAA in DMSO-d_6 with $w_{mon,0}$ = 0.5 ($\triangle$) and 0.1 ($\bigcirc$). Lines are simulated using the best-fit reactivity ratio estimated from corresponding data set.

MAA data set. However, there is a significant difference between the best fit values, especially r_{MAA}, for the two data sets. Thus, unlike for MA/DEGMEMA, overall monomer concentration affects copolymer composition for MA/MAA copolymerized in DMSO-d_6, such that the data cannot be well-represented by a single pair of values.

While both the r_{MAA} and r_{MA} values are higher for w_{mon} = 0.5 compared to 0.1, the increase in r_{MAA} is much greater. This observation can be explained by consideration of competitive complexation between the MAA carboxyl functionally with itself (*i.e.*, dimerization), and with the electron-donor solvent DMSO-d_6. As shown in Fig. 7, both interactions decrease the electron density on the vinylic bond. However, DMSO-d_6 is an aprotic (electron-donor) solvent which results in a net decrease in r_{MAA} as DMSO-d_6 content increases due to the balance between two competing influences: the formation of a π-complex between the acid radical and DMSO-d_6 reduces MAA addition relative to MA, while formation of H-complexes between the monomer and the solvent facilitates it.[35] Moreover, the lower enthalpy of MAA dimerization compared to its hydrogen bonding to DMSO-d_6 increases the probability
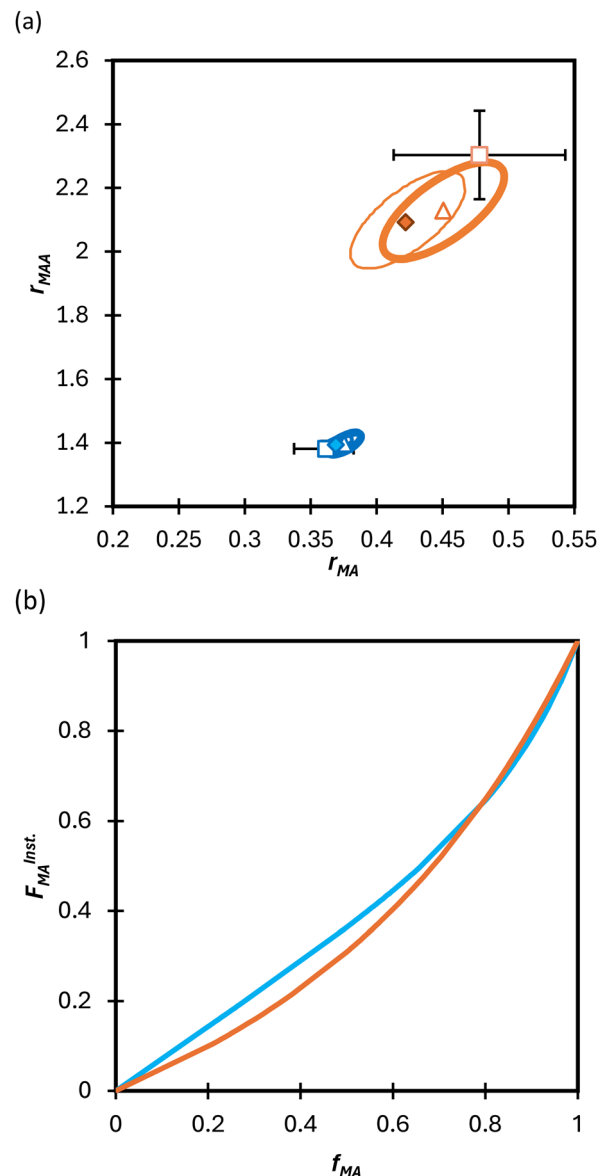
Fig. 6 (a) 95% joint confidence regions from estimation of the reactivity ratios and (b) $F_{MA}^{Inst.}$ *vs.* f_{MA} calculated for the copolymerization of MA/MAA in DMSO-d_6 with w_{mon} = 0.5 (orange) and 0.1 (blue). The JCRs were obtained by different parameter estimation techniques (see Table 2 and text): ML (solid thicker lines with $\triangle$ indicating best-fit values), Contour (solid thinner lines, $\blacklozenge$), and DNI ($\square$, with error bars). F_{MA}^{Inst} is derived using estimated reactivity ratios from the DNI fit.

Table 2 Reactivity ratios (with 95% confidence intervals) for the copolymerization of MA/MAA in DMSO-d_6 estimated using three different methodologies

| $w_{mon,0}$ | DNI | | Meyer-Lowry | | Contour | |
	r_{MA}	r_{MAA}	r_{MA}	r_{MAA}	r_{MA}	r_{MAA}
0.5	0.48 ± 0.06	2.30 ± 0.14	0.45 ± 0.02	2.13 ± 0.06	0.42 ± 0.02	2.10 ± 0.08
0.1	0.36 ± 0.02	1.38 ± 0.02	0.37 ± 0.01	1.40 ± 0.01	0.37 ± 0.01	1.39 ± 0.01

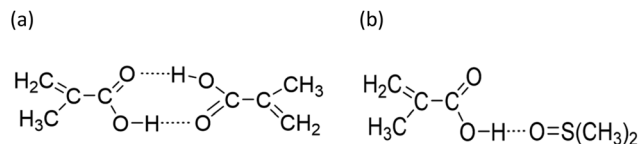(a)   (b)

Fig. 7 Proposed complexation between methacrylic acid and (a) itself, *i.e.*, dimerization, and (b) H-bounding between MAA and DMSO.

of dimerization as w_{mon} increases, thus increasing the relative incorporation of MAA to MA to the copolymer and the value of r_{MAA}. Comparing the reactivity ratio of MA/MAA (Table 2) with MA/DEGMEMA (Table 1) reveals that the best-fit value for MA/DEGMEMA ($r_{DEGMEMA}$ = 2.16, Table 1) is between the two MA/MAA estimates (r_{MAA} = 1.38 for w_{mon} = 0.1 and 2.30 for w_{mon} = 0.5, Table 2). As a non-functional monomer, DEGMEMA does not participate in dimerization or complex formation, thus showing no dependence on monomer concentration in DMSO-d$_6$.

Copolymerization in aqueous solution

Moving towards aqueous solution, a series of *in situ* NMR experiments have been performed for both comonomer systems in a solvent mixture of D$_2$O : EtOD (α_{EtOD} = 0.5). To study the effect of solvent concentration, $w_{mon,0}$ was varied between 0.05 and 0.5 for MA/MAA, with all solutions remaining homogeneous over the complete range of conversion. As shown in Fig. 8(a), the increase in f_{MA} with conversion is independent of $w_{mon,0}$. Although there were slight variations in the estimated values of r summarized in Table 3, no systematic variation in either r_{MAA} or r_{MA} was observed as the solution was diluted from $w_{mon,0}$ = 0.5 to 0.05. As demonstrated in Fig. 8(a), the composition drifts are well represented by a single pair of values, r_{MAA} = 2.17 ± 0.01 and r_{MA} = 0.28 ± 0.01, estimated from a fit of the combined data set. While corresponding MA/DEGMEMA data were only collected for $w_{mon,0}$ = 0.5 and 0.1, the same conclusion can be drawn: the measured drifts in f_{MA} shown in Fig. 8(b) are well-fit with $r_{DEGMEMA}$ = 2.37 ± 0.01 and r_{MA} = 0.27 ± 0.01 (Table 3).

Not only are the composition drifts independent of monomer level for both MA/MAA and MA/DEGMEMA in the polar D$_2$O : EtOD mixture, the F_{MA} *vs.* f_{MA} curves for the two systems almost overlap, as shown in Fig. 9. In addition, the best-fit reactivity ratios are very similar to those reported for the copolymerization of MEA with HEMA in alcohol/water mixtures, r_{HEMA} = 2.4 ± 0.2 and r_{MEA} = 0.28 ± 0.02;[20] the values in that study were estimated from the fitting of eqn (3) to low conversion f–F data, with the larger uncertainty arising from the reduced number of datapoints. The results support the conclusion that the copolymerization behavior of all methacrylate–acrylate systems – whether functional (*e.g.*, HEMA or MAA) or non-functional (DEGMEMA; MA or MEA) – becomes uniform in protic polar aqueous solution, even though differences are seen when copolymerization behavior is compared to bulk,[20] or in solvents such as toluene-d$_8$ and DMSO-d$_6$ (Fig. 9). It is notable that switching from DMSO-d$_6$ or toluene-d$_8$ to D$_2$O : EtOD has little influence on MA/DEGMEMA copoly-

(a)

(b)

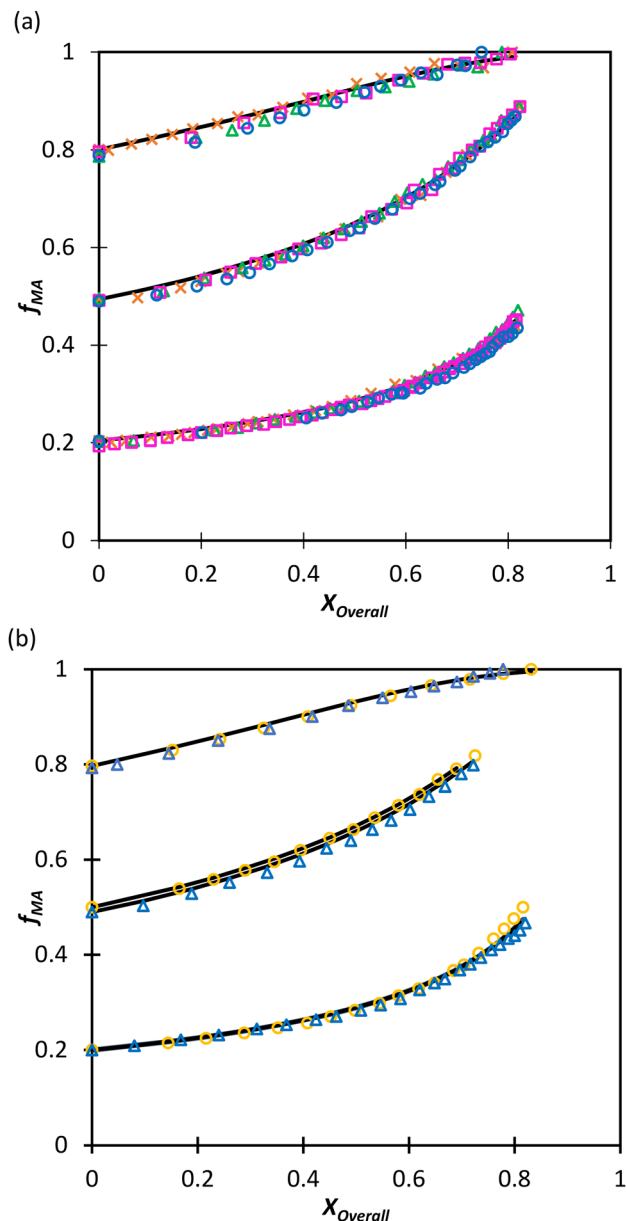**Fig. 8** Drift in MA comonomer composition (f_{MA}) with overall monomer conversion for copolymerization of MA in D$_2$O : EtOD with α_{EtOD} = 0.5 with: (a) MAA and $w_{mon,0}$ of 0.50 (×), 0.20 (△), 0.10 (□) and 0.05 (○); (b) DEGMEMA with $w_{mon,0}$ = 0.50 (△) and 0.10 (○). Lines are calculated using the reactivity ratios fits estimated from the combined data sets for each system (see Table 3). α_{EtOD} refers to wt% of EtOD in D$_2$O : EtOD mixture.

mer composition, suggesting that the H-bonding introduced by the solvent affects both monomers equally. In contrast, DMSO-d$_6$ and the aqueous solution influence the relative reactivities of MAA and MA to a different extent, resulting in an observable shift in copolymer composition in the two solvents, as also seen when comparing the bulk MEA/HEMA to its copolymerization behavior in alcohol/water mixtures.[20]

Extrapolation of these conclusions suggests that the Table 3 values of $r_{methacrylate}$ = 2.2–2.4 and $r_{acrylate}$ = 0.28 ± 0.02 should
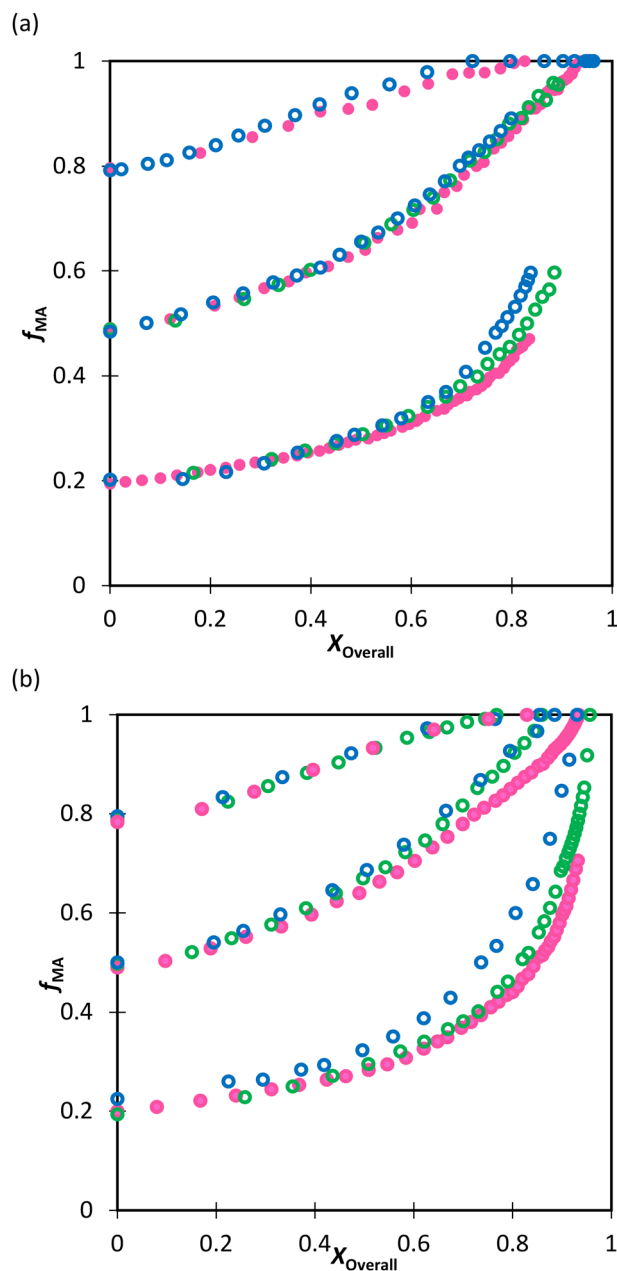
Table 3 Reactivity ratios (with 95% confidence intervals) for the copolymerizations of MA with MAA and DEGMEMA in D_2O : EtOD with $\alpha_{EtOD} = 0.5$

$w_{mon,0}$	MA/MAA		MA/DEGMEMA	
	r_{MA}	r_{MAA}	r_{MA}	$r_{DEGMEMA}$
0.5	0.27 ± 0.02	2.11 ± 0.06	0.27 ± 0.04	2.56 ± 0.08
0.2	0.28 ± 0.02	2.22 ± 0.04	NA	NA
0.1	0.30 ± 0.01	2.34 ± 0.03	0.27 ± 0.02	2.28 ± 0.03
0.05	0.26 ± 0.02	1.97 ± 0.03	NA	NA
Combined data	0.28 ± 0.01	2.17 ± 0.03	0.27 ± 0.03	2.37 ± 0.05
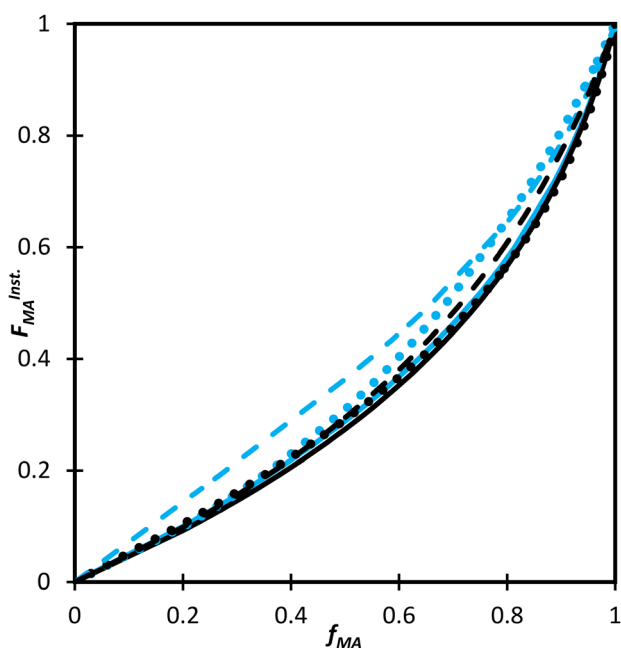
Fig. 9 F_{MA}^{Inst} vs. f_{MA} calculated for the copolymerization of: MA/MAA (blue) and MA/DEGMEMA (black) in D_2O : EtOD ($\alpha_{EtOD} = 0.5$) (solid line) and in DMSO-d_6 with $w_{mon,0} = 0.50$ (dots) and $w_{mon,0} = 0.10$ (dashed). α_{EtOD} refers to wt% of EtOD in D_2O : EtOD mixture.

Fig. 10 Drift in MA comonomer composition (f_{MA}) with overall monomer conversion for its copolymerization in D_2O : EtOD for $w_{mon,0} = 0.10$ and $\alpha_{EtOD} = 0.5$ (pink), 0.25 (green), and 0.1 (blue) with (a) MAA and (b) DEGMEMA. Filled points refer to homogeneous samples at the end of *In situ* NMR. α_{EtOD} refers to wt% of EtOD in D_2O : EtOD mixture.

capture the relationship between comonomer and copolymer composition for any acrylate/methacrylate system, including BA/MMA, in polar solution, including aqueous systems. To test this hypothesis, the fraction of water in the D_2O : EtOD solvent mixture was increased from $\alpha_{EtOD} = 0.5$ to $\alpha_{EtOD} = 0.25$ and 0.10, with $w_{mon,0}$ set to 0.10. The drifts in f_{MA} measured for both the MA/MAA (Fig. 10(a)) and MA/DEGMEMA (Fig. 10(b)) systems, indicate that the MAA or DEGMEMA comonomer is consumed more quickly moving from $\alpha_{EtOD} = 0.5$ to 0.1 (*i.e.*, f_{MA} increases towards unity at lower conversion), with the change more significant for $f_{MA,0} = 0.2$ than $f_{MA,0} = 0.8$. However, the copolymer precipitated out of solution as the water fraction in the mixed solvent was increased, with turbidity observed after removing the samples from the NMR chamber and, in some cases, loss of shimming during the acquisition. Thus, the possibility of monomers partition-

ing and polymerizing in the two phases cannot be ruled out, and reactivity ratios were not estimated from the experiments with $\alpha_{EtOD} = 0.25$ and 0.1. A follow-up study is planned to directly measure copolymer composition from low-conversion experiments to determine whether the measured compositions differ significantly with decreased α_{EtOD} from those calculated using the reactivity ratios determined in this *in situ* NMR study.

Effect of solvent on copolymerization rates

While the focus of this study is the influence of solvent and methacrylate functionality on monomer reactivity ratios, insights can be also gained by analyzing how the reaction conditions influence the rates of overall monomer conversion. Assuming a constant volume batch reaction, radical stationarity, and negligible side reactions, the rate of monomer conversion can be written as:

$$\frac{dX}{dt} = k_p(1-X)\left(\frac{2fk_d[I]}{k_t}\right)^{0.5} \quad (5)$$

Eqn (5) can be integrated assuming that the copolymerization kinetic rate coefficients are constant with conversion, to yield the lumped rate coefficient $k_p^{cop}/(k_t^{cop})^{0.5}$:

$$\frac{k_p^{cop}}{(k_t^{cop})^{0.5}} = \frac{\ln(1-X)}{(\exp(-0.5k_dt)-1)}\left(\frac{k_d}{8[I]_0f}\right)^{0.5} \quad (6)$$

where X refers to overall monomer conversion, k_d is the initiator decomposition rate with the value of 1×10^{-5} s^{-1} and 3×10^{-5} s^{-1} for AIBN[36] and V-50[37] at 60 °C, respectively, and initiator efficiency, f, is set to 0.8.[38] For a copolymerization system, the propagation (k_p^{cop}) and termination (k_t^{cop}) rate coefficients will both vary with comonomer composition. However, it can be generally assumed that the variation in their ratio is mainly an indication of a change in k_p^{cop}; as a diffusion-controlled rate coefficient, k_t^{cop} is largely a function of solution viscosity.[39,40]

The calculated lumped values for MA/MAA copolymerization in DMSO-d$_6$ and D$_2$O : EtOD (α_{EtOD} = 0.5) are plotted against overall monomer conversion in Fig. 11(a) and (b) for $w_{mon,0}$ = 0.1 and 0.5, respectively. The curves are relatively flat for $w_{mon,0}$ = 0.1 but show a slight and consistent increase with

increasing monomer conversion for $w_{mon,0}$ = 0.5. This difference is attributed to the Trommsdorff effect,[41,42] with the increased viscosity of the polymerizing system containing 50 wt% monomer with conversion causing a decrease in k_t[43] and therefore an increase in the $k_p/k_t^{0.5}$ ratio. The monomer conversion profiles shown as Fig. S9† demonstrate an acceleration in the rate of conversion with time, consistent with this interpretation. However, a systematic variation of k_p^{cop} with conversion cannot be ruled out. Assuming terminal model kinetics, the composition-averaged value is a function of the two homopropagation rate coefficients as well as the system reactivity ratios:

$$k_p^{cop} = \frac{r_1f_1^2 + 2f_1f_2 + r_2f_2^2}{(r_1f_1/k_{p_{11}}) + (r_2f_2/k_{p_{22}})} \quad (7)$$

As homopropagation k_p values for acrylates are ~50 times higher than methacrylates,[44] the increase in f_{MA} with conversion (Fig. 5 and 8a) will also lead to an increase in k_p^{cop}. Note that changes in either value with conversion violates the "constant coefficient" assumption made when integrating eqn (5) to obtain eqn (6). Thus, we restrict ourselves to qualitative discussion of the observed trends.

With the exception of $f_{MA,0}$ = 0.8 with $w_{mon,0}$ = 0.5 in Fig. 11b, the polymerization rates are higher in D$_2$O : EtOD than in DMSO-d$_6$, consistent with previous results showing that k_p^{cop} values are elevated in alcohol/water mixtures.[16] Furthermore, as expected from eqn (7), the $k_p/(k_t)^{0.5}$ ratio increases as the MA fraction is increased from $f_{MA,0}$ = 0.2 to 0.8. It is interesting to note that the relative increase is quite system dependent; the relative change in $k_p/(k_t)^{0.5}$ with $f_{MA,0}$ in D$_2$O : EtOD is much larger for $w_{mon,0}$ = 0.1 (Fig. 11a) than for $w_{mon,0}$ = 0.5 (Fig. 11b) for the MA/MAA system.
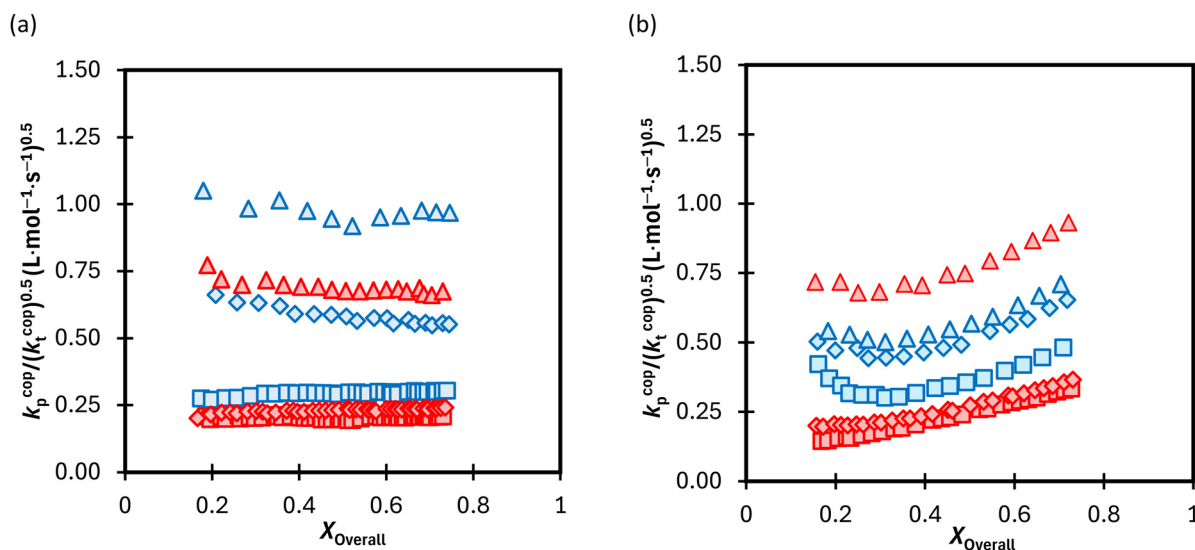
Fig. 11 (a) Calculated lumped rate coefficient ($k_p^{cop}/(k_t^{cop})^{0.5}$) vs. conversion for the copolymerization of MA–MAA at 60 °C with (a) $w_{mon,0}$ = 0.1 and (b) $w_{mon,0}$ = 0.5 with monomer ratio of 20 : 80 (□), 50 : 50 (◇) and 80 : 20 (△) (mol : mol) in DMSO-d$_6$ (red) vs. D$_2$O : EtOD (α_{EtOD} = 0.5) (blue). α_{EtOD} refers to wt% of EtOD in D$_2$O : EtOD mixture.
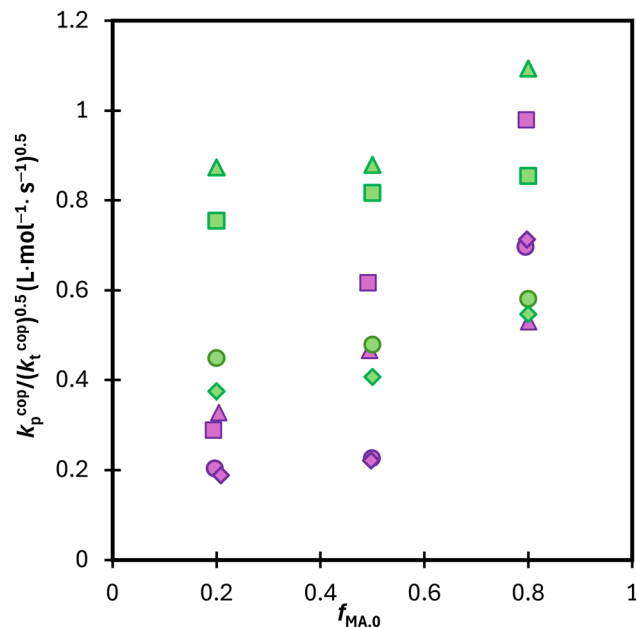
Fig. 12 Calculated average lumped rate coefficient ($k_p^{cop}/(k_t^{cop})^{0.5}$) from data presented in Fig. 11 and S10† from conversion 0.15–0.5 for MA–MAA (purple) and MA–DEGMEMA (green) with w_{mon} = 0.5 in DMSO-d_6 (◇), w_{mon} = 0.1 in DMSO-d_6 (○), w_{mon} = 0.5 in D$_2$O : EtOD (△) and w_{mon} = 0.5 in D$_2$O : EtOD (□) with α_{EtOD} = 0.5. α_{EtOD} refers to wt% of EtOD in D$_2$O : EtOD mixture.

The same analysis was completed for the MA/DEGMEMA conversion profiles measured in DMSO-d_6 and D$_2$O : EtOD, as summarized in Fig. S10.† Results for the two systems are compared in Fig. 12, with the average $k_p/(k_t)^{0.5}$ values calculated from data in the 0.15 to 0.50 conversion range to minimize the influence of changing k_p^{cop} (due to changing f_{MA}) and/or k_t (due to the Trommsdorff effect). For all systems with $f_{MA,0}$ = 0.2 and 0.5, polymerization is faster in MA/DEGMEMA (*i.e.*, higher $k_p/(k_t)^{0.5}$) than the corresponding MA/MAA system. This result may be explained by a lowered k_t value for DEGMEMA compared to MAA because of the bulkier monomer.[15] However, the opposing behavior – a higher $k_p/(k_t)^{0.5}$ value for MA/MAA than MA/DEGMEMA – is seen for some solvent conditions with $f_{MA,0}$ = 0.8. A more complete interpretation of these trends, including evaluating the suitability of terminal model kinetics to represent k_p^{cop},[22,23] will be possible once k_p^{cop} is directly measured by PLP/SEC (pulsed-laser polymerization combined with size exclusion chromatography analysis), a study that is currently underway. Nonetheless, it is clear from this analysis that copolymerization rates are strongly influenced by both solvent composition and overall comonomer concentration, in contrast to the weak dependencies observed in comonomer reactivity ratios.

Conclusions

In situ NMR is used to study the solution radical copolymerization of MA with MAA and DEGMEMA in deuterated DMSO and ethanol–water mixtures at 60 °C up to high conversions. The

drift in f_{MA} with overall monomer conversion was employed to estimate reactivity ratios, with good agreement in the best-fit values found using three different methodologies. While small variations with monomer concentration cannot be ruled out, the experimental data are well-fit using a single pair of reactivity ratios for MA/DEGMEMA in DMSO-d_6 and toluene-d_8, for MA/DEGMEMA in D$_2$O : EtOD (α_{EtOD} = 0.5), and for MA/MAA in D$_2$O : EtOD (α_{EtOD} = 0.5). Switching from DMSO-d_6 or toluene-d_8 to D$_2$O : EtOD has little influence on MA/DEGMEMA copolymer composition, suggesting that the H-bonding introduced by the solvent affects both monomers equally. However, there was a significant influence of monomer concentration on the r values for MA/MAA in DMSO-d_6, explained by competitive solvent-monomer and monomer–monomer complexation involving the carboxyl functionality of MAA.

The copolymer composition plots for MA/MAA and MA/DEGMEMA in the polar D$_2$O : EtOD mixture are not only independent of monomer concentration, the curves for the two systems almost overlap. Supported by other literature, the results support the conclusion that the copolymerization behavior of all methacrylate–acrylate systems – whether involving functional or non-functional monomers – becomes uniform in protic polar aqueous solution, even though differences are seen when copolymerization behavior is compared to bulk or in solvents such as toluene and DMSO. Thus, values of $r_{methacrylate}$ = 2.2–2.4 and $r_{acrylate}$ = 0.28 ± 0.02 should capture the relationship between comonomer and copolymer composition for any acrylate/methacrylate system in polar solution, including BA/MMA in emulsion systems. In contrast to the weak dependencies observed in comonomer reactivity ratios, however, the overall rates of conversion are strongly influenced by comonomer choice (MAA *vs.* DEGMEMA), solvent composition, and overall comonomer concentration. The validity of these conclusions as the system is moved toward pure water will be examined by measuring copolymer composition and k_p^{cop} values at low conversion using the PLP/SEC technique.

Data availability

The best-fit reactivity ratios measured in this study are summarized in Tables 1–3. NMR data supporting this article have been included as part of the ESI.†

Author contributions

Conflicts of interest

There are no conflicts to declare.

References

1 P. A. Lovell and F. J. Schork, Fundamentals of Emulsion Polymerization, *Biomacromolecules*, 2020, **21**, 4396–4441.

2 *Polymer Colloids Formation, Characterization and Applications*, ed. R. D. Priestley and R. Prud'homme, The Royal Society of Chemistry, 2020.

3 D. Urban, B. Schuler and J. Schmidt-Thummes, in *Chemistry and technology of emulsion polymerisation*, ed. A. M. van Herk, Wiley, UK, 2nd edn, 2013, p. 347.

4 M. Aguirre, N. Ballard, E. Gonzalez, S. Hamzehlou, H. Sardon, M. Calderon, M. Paulis, R. Tomovska, D. Dupin, R. H. Bean, T. E. Long, J. R. Leiza and J. M. Asua, Polymer Colloids: Current Challenges, Emerging Applications, and New Developments, *Macromolecules*, 2023, **56**, 2579–2607.

5 J. M. Asua, A new model for radical desorption in emulsion polymerization, *Macromolecules*, 2003, **36**, 6245–6251.

6 H. M. Vale and T. F. Mckenna, Particle formation in vinyl chloride emulsion polymerization: Reaction modeling, *Ind. Eng. Chem. Res.*, 2009, **48**, 5193–5210.

7 J. P. A. Heuts and G. T. Russell, The nature of the chain-length dependence of the propagation rate coefficient and its effect on the kinetics of free-radical polymerization. 1. Small-molecule studies, *Eur. Polym. J.*, 2006, **42**, 3–20.

8 W. V. Smith and R. H. Ewart, Kinetics of Emulsion Polymerization Kinetics of Emulsion Polymerization, *J. Chem. Phys.*, 1948, **16**, 592–599.

9 F. K. Hansen and J. Ugelstad, Particle Nucleation in Emulsion Polymerization - 1. a Theory for Homogeneous Nucleation., *J. Polym. Sci., Polym. Chem. Ed.*, 1978, **16**, 1953–1979.

10 M. Zubitur, P. D. Armitage, S. Ben Amor, J. R. Leiza and J. M. Asua, Mathematical modeling of multimonomer (vinylic, divinylic, acidic) emulsion copolymerization systems, *Polym. React. Eng.*, 2003, **11**, 627–662.

11 J. Herrera-Ordonez, C. L. Azanza Ricardo and D. Victoria-Valenzuela, On the diffusive step of free-radical entry in emulsion polymerization and the applicability of the Smoluchowski rate coefficient, *Colloids Surf., A*, 2018, **556**, 134–139.

12 P. Daswani and A. Van Herk, Entry in emulsion copolymerization: Can the existing models be verified?, *Macromol. Theory Simul.*, 2011, **20**, 614–620.

13 S. Beuermann, M. Buback, P. Hesse and I. Lacík, Free-radical propagation rate coefficient of nonionized methacrylic acid in aqueous solution from low monomer concentrations to bulk polymerization, *Macromolecules*, 2006, **39**, 184–193.

14 I. Refai, M. Agboluaje and R. A. Hutchinson, Radical copolymerization kinetics of N-tert -butyl acrylamide and methyl acrylate in polar media, *Polym. Chem.*, 2022, **13**, 2036–2047.

15 M. Buback, R. A. Hutchinson and I. Lacík, Radical polymerization kinetics of water-soluble monomers, *Prog. Polym. Sci.*, 2023, **138**, 101645.

16 M. Agboluaje, I. Refai, H. H. Manston, R. A. Hutchinson, E. Dušička, A. Urbanová and I. Lacík, A comparison of the solution radical propagation kinetics of partially water-miscible non-functional acrylates to acrylic acid, *Polym. Chem.*, 2020, **11**, 7104–7114.

17 S. Hamzehlou, Y. Reyes and J. R. Leiza, Modeling the Mini-Emulsion Copolymerization of *N* -Butyl Acrylate with a Water-Soluble Monomer: A Monte Carlo Approach, *Ind. Eng. Chem. Res.*, 2014, **53**, 8996–9003.

18 G. S. Georgiev and I. G. Dakova, Solvent effect on the methacrylic acid-methyl methacrylate radical copolymerization. Analytical estimation by linear and nonlinear solvation energy relationships, *Macromol. Chem. Phys.*, 1994, **195**, 1695–1707.

19 G. A. Stahl, Copolymerization Parameters of Methyl Methacrylate and Acrylic Acid, *J. Polym. Sci., Part A-1: Polym. Chem.*, 1981, **19**, 371–380.

20 M. Agboluaje and R. A. Hutchinson, The effect of hydrogen bonding on the copolymerization kinetics of 2-methoxyethyl acrylate with 2-hydroxyethyl methacrylate in alcohol and aqueous solutions, *Can. J. Chem. Eng.*, 2022, **100**, 689–702.

21 L. A. Idowu and R. A. Hutchinson, Solvent Effects on Radical Copolymerization Kinetics of 2-Hydroxyethyl Methacrylate and Butyl Methacrylate, *Polymers*, 2019, **11**, 487.

22 J. E. S. Schier, D. Cohen-Sacal and R. A. Hutchinson, Hydrogen bonding in radical solution copolymerization kinetics of acrylates and methacrylates: a comparison of hydroxy- and methoxy-functionality, *Polym. Chem.*, 2017, **8**, 1943–1952.

23 J. E. S. Schier and R. A. Hutchinson, The influence of hydrogen bonding on radical chain-growth parameters for butyl methacrylate/2-hydroxyethyl acrylate solution copolymerization, *Polym. Chem.*, 2016, **7**, 4567–4574.

24 P. Deglmann, K. Hungenberg and H. M. Vale, Dependence of Copolymer Composition in Radical Polymerization on Solution Properties: a Quantitative Thermodynamic Interpretation, *Ind. Eng. Chem. Res.*, 2021, **60**, 10566–10583.

25 P. Daswani and A. van Herk, Selective Adsorption of Aqueous Phase Co-Oligomers on Latex Particles Part 1: Influence of Different Initiator Systems, *Macromol. Theory Simul.*, 2017, **26**, 1600047.

26 K. Ouzineb, M. Fortuny Heredia, C. Graillat and T. F. Mckenna, Stabilization and kinetics in the emulsion copolymerization of butyl acrylate and methyl methacrylate, *J. Polym. Sci., Part A: Polym. Chem.*, 2001, **39**, 2832–2846.

27 M. Agboluaje and R. A. Hutchinson, Measurement and Modeling of Methyl Acrylate Radical Polymerization in Polar and Nonpolar Solvents, *Ind. Eng. Chem. Res.*, 2022, **61**, 6398–6413.

28 S. S. Cutié, D. E. Henton, C. Powell, R. E. Reim, P. B. Smith and T. L. Staples, The Effects of MEHQ on the Polymerization of Acrylic Acid in the Preparation of Superabsorbent Gels, *J. Appl. Polym. Sci.*, 1997, **64**, 577–589.

29 B. Mbergen, W. Heitler, E. Teller, P. Roy Soc, E. M. Purcell, H. C. Torrey, R. V. Pound, B. Rollin, J. Hatton, A. H. Cooke and R. J. Benzie, Relaxation Effects in Nuclear Magnetic Resonance Absorption, *Phys. Rev.*, 1948, **73**, 679–711.

30 C. Preusser and R. A. Hutchinson, An *In situ* NMR Study of Radical Copolymerization Kinetics of Acrylamide and Non-Ionized Acrylic Acid in Aqueous Solution, *Macromol. Symp.*, 2013, **333**, 122–137.

31 N. Kazemi, T. A. Duever and A. Penlidis, Reactivity Ratio Estimation from Cumulative Copolymer Composition Data, *Macromol. React. Eng.*, 2011, **5**, 385–403.

32 A. A. A. Autzen, S. Beuermann, M. Drache, C. M. Fellows, S. Harrisson, A. M. Van Herk, R. A. Hutchinson, A. Kajiwara, D. J. Keddie, B. Klumperman and G. T. Russell, IUPAC recommended experimental methods and data evaluation procedures for the determination of radical copolymerization reactivity ratios from composition data, *Polym. Chem.*, 2024, **15**, 1851–1861.

33 V. E. Meyer and G. G. Lowry, Integral and Differential Binary Copolymerization Equations, *J. Polym. Sci., Part A: Gen. Pap.*, 1965, **3**, 2843–2851.

34 A. L. Burke, T. A. Duever and A. Penlidis, Revisiting the design of experiments for copolymer reactivity ratio estimation, *J. Polym. Sci., Part A: Polym. Chem.*, 1993, **31**, 3065–3072.

35 R. Makuška, G. I. Bayoras, Y. K. Shulskus, A. B. Bolotin, Z. A. Roganova and A. L. Smolyanskii, Effect of complex formation on reactivity of acrylic and methacrylic acids in

radical polymerization, *Polym. Sci. U.S.S.R.*, 1985, **27**, 634–641.

36 AIBN|CAS:78-67-1|2,2′-Azobis(isobutyronitrile)|FUJIFILM Wako Chemicals U.S.A. Corporation, **https://specchem-wako.fujifilm.com/us/oil-soluble-azo-initiators/AIBN.htm**, (accessed 23 May 2024).

37 V-50|CAS:2997-92-4|2,2′-Azobis(2-methylpropionamidine) dihydrochloride|AAPH|FUJIFILM Wako Chemicals U.S.A. Corporation, **https://specchem-wako.fujifilm.com/us/water-soluble-azo-initiators/V-50.htm**, (accessed 23 May 2024).

38 I. H. Ezenwajiaku, A. Chovancová, K. C. Lister, I. Lacík and R. A. Hutchinson, Experimental and Modeling Investigation of Radical Homopolymerization of 2-(Methacryloyloxyethyl) Trimethylammonium Chloride in Aqueous Solution, *Macromol. React. Eng.*, 2020, **14**, 1900033.

39 G. A. O'Neil, M. B. Wisnudel and J. M. Torkelson, A critical experimental examination of the gel effect in free radical polymerization: Do entanglements cause autoacceleration?, *Macromolecules*, 1996, **29**, 7477–7490.

40 T. J. Tulig and M. Tirrell, On the Onset of the Trommsdroff effect, *Macromolecules*, 1982, **15**, 459–463.

41 E. Trommsdorff, H. Köhle and P. Lagally, For the polymerization of the methacrylic acid methyl ester, *Macromol. Chem.*, 1948, 169–198.

42 G. V. Schulz and G. Harborth, About the mechanism of the explosive polymerization course of the methacrylic acid methyl ester, *Macromol. Chem.*, 1947, 106–139.

43 P. Zhan, J. Chen, A. Zheng, H. Shi, F. Chen, D. Wei, X. Xu and Y. Guan, The Trommsdorff effect under shear and bulk polymerization of methyl methacrylate via reactive extrusion, *Eur. Polym. J.*, 2020, **122**, 109272.

44 S. Beuermann, S. Harrisson, R. A. Hutchinson, T. Junkers and G. T. Russell, Update and critical reanalysis of IUPAC benchmark propagation rate coefficient data, *Polym. Chem.*, 2022, **13**, 1891–1900.